34th Annual International Conference of the IEEE EMBS
San Diego, California USA, 28 August - 1 September, 2012

Stable Online Control of an Electrocorticographic Brain-Computer Interface using a Static Decoder

Robin C. Ashmore, Bridget M. Endler, Ivan Smalianchuk, Alan D. Degenhart, Nicholas G. Hatsopoulos, Elizabeth C. Tyler-Kabara, Aaron P. Batista, Wei Wang

***Abstract*—A brain computer interface (BCI) system was implemented by recording electrocorticographic signals (ECoG) from the motor cortex of a Rhesus macaque. These signals were used to control two-dimensional cursor movements in a standard center-out task, utilizing an optimal linear estimation (OLE) method. We examined the time course over which a monkey could acquire accurate control when operating in a co-adaptive training scheme. Accurate and maintained control was achieved after 4-5 days. We then held the decode parameters constant and observed stable control over the next 28 days. We also investigated the underlying neural strategy employed for control, asking whether neural features that were correlated with a given kinematic output (e.g. velocity in a certain direction) were clustered anatomically, and whether the features were coordinated or conflicting in their contributions to the control signal.**

I. Introduction

Electrocorticography (ECoG) holds promise as a technique for implementing brain-computer interface (BCI) and neural prosthetic control systems. The primary advantages of ECoG are its minimally invasive nature (as opposed to penetrating electrodes), and its hypothesized stability over time (see [1] for review). Since ECoG electrodes record signals from large populations of neurons, these recordings are not dependent upon the integrity and reliability of individual cells. As such, BCI systems based on ECoG may remain robust and stable, without the need for daily updating and retraining of decoders. One possible disadvantage of an ECoG-based system is the potential challenge presented to a user learning to operate it. While individual neurons in motor cortical areas are often highly tuned to intended movement direction [2][3][4][5][6], broad populations may not present the same level of resolution when recorded in the aggregate. The distributed representation of movement parameters recordable at the single unit level may not be accessible in an ECoG-based BCI. Alternatively, a more artificial control strategy, perhaps based on broad somatotopic anatomical divisions, may be necessary to achieve accurate control [7].

Previous studies have begun to address these issues, producing generally encouraging results. Chao et al. [8] demonstrated that ECoG signals can retain both their magnitude and representational content over long periods. Other studies have demonstrated that humans can learn to intentionally modulate ECoG signals for the purpose of 1D [9] or 2D [7] cursor control. Rouse and Moran [10] showed that monkeys can learn to de-correlate epidural ECoG signals from 2 arbitrarily chosen electrodes to gain 2D cursor control. It has also been shown that ECoG signals can contain highly accurate information about the details of performed movements [11][12][13][14][15]. These studies support the feasibility of extracting natural control signals from ECoG recordings and suggest that implementation of a robust, learnable, and intuitive ECoG-based BCI system is a viable goal.

In this study we focus on three aspects of ECoG-based BCI control. First, we address learnability by examining the time course to acquire 2D cursor control with a neural decoder utilizing a large number of ECoG signal features. Second, to examine stability we froze our BCI decoder and observed performance over multiple days. Third, we explored the strategy the animal employed to control the decoder by examining which neural features, and by extension which cortical areas, contributed substantially to cursor control.

II. Materials and Methods

A. Surgery and Implant

All procedures described here were approved by the Institutional Animal Care and Use Committee of the University of Pittsburgh and were in accordance with the National Institutes of Health's Guidelines for the Care and Use of Laboratory Animals. Briefly, a male Rhesus macaque (*mucaca mulatta*) was anesthetized, and a craniotomy was opened over the left motor and premotor cortex. The dura was peeled back to expose an area approximately 2x2 cm between the arcuate and central sulci. A custom-built 15-channel ECoG grid (PMT Corp, Chanhassen, MN, USA) was placed directly on the exposed brain surface (Fig. 1), and the dura and the bone were reapproximated. Wires from the grid were connected to a Cereport pedestal connector (Blackrock Microsystems) affixed to the skull.

*Research supported by National Institutes of Health (NIH) Grants 3R01NS050256-05S1, KL2 RR024154. SPAWAR under Contract No N66001-10-C-4056 20100630, Telemedicine and Advanced Technology Research Center of the US Army Medical Research and Materiel Command Agreement W81XWH-07-1-0716, by the Burroughs Wellcome Fund, CRCNS NICHD/NSF R01 HD071686, NINDS R01 NS065065, and the Craig H. Neilsen Foundation.

R. C. Ashmore, B M. Endler, I. Smalianchuk, A. D. Degenhart, E. C. Tyler-Kabara, A. P. Batista, and W. Wang are with the University of Pittsburgh, Pittsburgh, PA.

N. G. Hatsopoulos is with the University of Chicago, Chicago, IL.

B. Neural Recording and Decoding

Signals from the ECoG grid were recorded with a g.USBamp Biosignal Amplifier (g.tec Medical Engineering), and sampled at 1200 Hz. The signals were filtered and processed using the Craniux Brain Computer Interface system [16]. Spectral estimation was performed using the Burg AR method [17] over the 40 to 180 Hz range (25th order, 10 Hz band width). These gamma and high gamma bands were chosen because they are typically spatially localized and informative about underlying neural processes [18][19][20]. Estimates were calculated every 33 ms using a sliding window of 300 ms of raw data. AR data were log-transformed, then normalized to pseudo Z-scores relative to a baseline condition [16]. These spectral estimates for each frequency band were used as the neural features for BCI control. Of the 15 channels available on the grid, one was used for a ground (e13), one for reference (e4), and electrical connectivity to a third (e2) was lost before experiments began. These electrodes were removed from the neural feature set used for online control. The remaining features (12 electrodes x 14 bands = 168 in total) were used for training, decoding, and control.

The neural decoder part of the BCI system employed the optimal linear estimation (OLE) algorithm [21] to determine a mapping between these neural features and cursor movement. This mapping took the form of a matrix of weights ($\boldsymbol{W}$) to be applied to the neural features ($\boldsymbol{f}$) for decoding, i.e. the two dimensions of cursor movement velocity ($\hat{v}$) were each a weighted sum of neural feature input, based on Equation 1. The decoding weights were calculated using the optimal linear estimator (OLE) algorithm based on Equation 2:

$$\hat{v} = fW \tag{1}$$

$$W = F^{+}V \tag{2}$$

where $\boldsymbol{V}$ and $\boldsymbol{F}$ are matrices representing the desired cursor movement direction and associated neural features, respectively. The desired cursor movement direction is the instantaneous unit vector pointing from the cursor to the target, averaged over a trial. The superscript "+" denotes pseudo-inverse of a matrix. Initial values for $\boldsymbol{V}$ and $\boldsymbol{F}$ were acquired from one block of trials where the monkey followed an automatically guided cursor with his hand. Each subsequent update of the decoder used all trials from a single block (see below).

C. Training and Task

The monkey was trained to perform an 8-target, center-out BCI-driven cursor task. The task was run in 40 trial blocks, and multiple blocks were run for each session (each testing day). At the start of each trial, a cursor appeared at the center of the computer screen in front of the monkey. Simultaneously, a pseudo-randomly selected target appeared, chosen from a set of 8 possible targets centered around the cursor starting position. During a 500 ms "hold" window immediately after target onset, the cursor was held fixed. Afterwards, the cursor was allowed to move under brain control. The monkey was required to move the cursor to the displayed target within 3 seconds. If the cursor overlapped with the target for 100-200 ms (randomly determined each trial), the trial was considered successful and the monkey was given an immediate water reward.

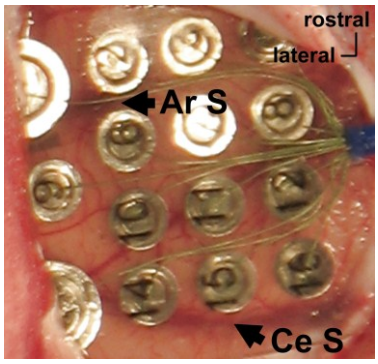

Figure 1. Placement of the ECoG grid over the left primary motor cortex (M1). The reference electrode (e4) and the ground (e13) are in the upper right and lower left, respectively.

Ar S: Arcuate sulcus.
Ce S: Central sulcus

Testing began on day 208 post-implant. In the initial testing sessions, the task software guided training for brain control by actively moving the cursor directly to the target ("active assist"). Following one fully assisted block (100% active assist) we trained the decoder, then reduced the amount of active assistance, that is, we computed a control signal that was a combination of the decoder output and the active assist. Over the course of multiple blocks (spanning multiple days) we lowered the amount of assistance incrementally (between blocks), until the cursor was under full brain control (0% active assist). The decision to lower the assist level was based on the success rate, such that high success rates over multiple blocks prompted a decrease in the assist level. Active assist was not used after session 7, thus success rates reported for subsequent sessions represent proficiency with full brain signal-derived control.

During the initial period of training, the decoding weights were updated periodically between blocks. Updates consisted of a blending of old and new weight values, such that changes in the decoder were gradual [22]. We refer to this process of adapting the decoder, simultaneous with continued learning on the part of the animal, as "Co-adaptation".

D. Analysis

To determine whether the success rate was above chance for trials without active assist, we performed a test using the neural data from the 440 trials of session 18 (chosen for the session's high mean success rate of 93.0%). We computed offline success rates using control signals generated from recorded ECoG signals and randomized decoder weights (decoder weights were randomly shuffled). Shuffled trials were considered successful if at any point during the trial the cursor intersected with the target. Shuffled success rates were generated 10000 times, yielding mean and maximum success rates of 12.3% and 28.6%, respectively. Since no shuffled value exceeded 28.6%, we used this success rate as a conservative estimate of chance accuracy.

We sought to quantify the accuracy of the control signals produced by the decoder. We computed for each trial the mean vector represented by the control signal (for trials with active assist, the calculation was done before the addition of

active assist), and compared it to the desired cursor movement vector pointing from the starting position to the target (Fig. 2B). To determine significance, the distribution of these angle differences over a block was compared to a shuffled version of the same data (control signals and target vectors were each drawn randomly without replacement from the same set of trials). Significance levels were determined by unpaired t-test.

In order to analyze the degree of spatial clustering of the kinematic output, we first separated trials by target location, and considered only successful trials. The contribution vectors, which are the combined components of the x- and y-decoder control signals for each neural feature, were calculated as the product of the static decoder weight for each feature and the normalized AR data derived from neural activity.

For each target direction, the control signal contribution vectors of each of the electrodes were summed across all features and all sampled time points during successful brain-controlled cursor movement, and then divided by the total number of time points for an average contribution from each electrode**.** This metric allowed for analysis across trials of varying duration. For each target direction, the net control signal was then calculated as the vector sum across all electrodes.

III. RESULTS

A. Training

The first step in training the BCI decoder was to present the center-out task for one block (40 trials) with 100% active assist (i.e., automatic computer control and no brain control). Subsequent to this first session, we ran partially-assisted trials, i.e. trials where the BCI output and the active assist were combined in varying ratios (Fig. 2A). During the first part of the training period (sessions 1 through 5), we gradually updated the decoder weights by retraining the decoder after 1~3 blocks, and blending the old and new weights together.

As shown in Fig. 2A, assistance was gradually lowered to 0% over the course of 7 sessions (spanning 8 days). However, the monkey began to exhibit significant control as early as the third day. To determine the accuracy of control, we computed the difference between the (unassisted) control signal vector produced by the BCI system and the starting point-to-target vector. Control signal vectors were significantly more accurate than chance ($p < 0.0005$) on blocks 2 and 3 of session 3. Significant vector accuracy was again seen on block 4 of session 4 ($p < 0.00001$), and this level of accuracy or higher was sustained from that point through the remainder of the study (Fig. 2B).

B. Sustained Performance

In total we ran 24 sessions spanning 33 days, beginning at day 208 post-implant. Following the removal of all active assist (set to 0% starting with session 8) and decoder updates (which ceased after session 5) we tracked the task success rate over multiple weeks (Fig. 2A). The mean success rate

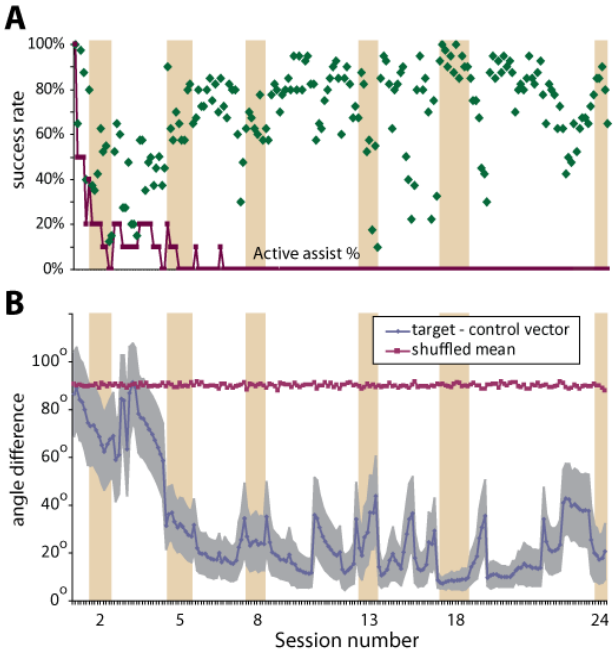

Figure 2. Performance measures over the course of all 24 sessions, spanning 33 days. Tan bars indicate sessions of interest described in the text. (A) The success rate for each block of 40 trials (green) is shown for all blocks run, along with the amount of active assist (red) employed for each block. (B) For each trial, the difference between the start-to-target vector and the vector sum of the control signals was computed. The mean angle difference for each block is shown (blue) surrounded by the 95% confidence interval (gray). The shuffled mean for each block (red) is shown for comparison.

for this first unassisted session was 70.6%, well above the significance threshold of 28.6% (see Methods for details). Over the course of the following 25 days, only 4 individual blocks had success rates that were not significant (for instance block 6, with 17.5%, and block 8 with 10%, for session 13). Note that these blocks of poor performance occurred on days where good performance was also seen (the maximum block success rate for session 13 was 87.5%), suggesting variable levels of engagement in the task, rather than an impaired ability to perform it.

C. Control Strategy

In order to investigate how the monkey modulated cortical activity to perform the task, we examined each feature's contribution to the control signal for horizontal (x) and vertical (y) dimensions (Fig. 3). Rightward movements appeared to have a strong contribution from a few electrodes (e.g. electrode e10, Fig. 3). To investigate this further, we analyzed the signal components by electrode and target direction (Fig. 4). For each direction and each electrode, we calculated a "contribution vector" as a measure of how strongly that electrode contributed to control in the target direction. As shown in Fig. 4, 5 of the 8 target directions had one strong rightward driver and several widely dispersed contribution vectors of smaller magnitude attenuating that signal. Conversely, the other targets had contribution vectors all of significantly smaller magnitude, but produced a comparable net control vector due to very few individual components in directions opposing the vector to the target.

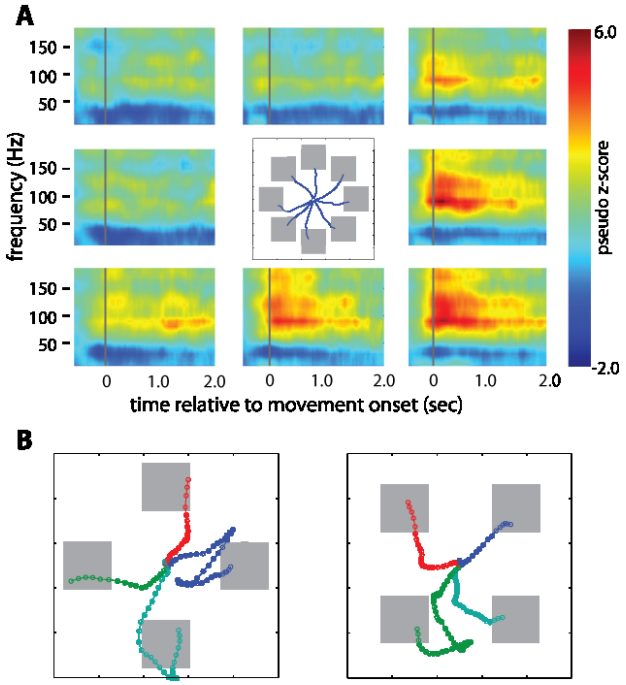

Figure 3. Neural and kinematic features. (A) The spectral estimates derived from the neural signals on one electrode (e10) are shown as time-frequency spectrograms, arranged by target direction. Data were taken from 200 trials (first 5 blocks of session 18), and each plot is an average of 25 trials. The center inset shows the mean paths for the same trials. (B) Representative trial paths for the four cardinal (left) and four diagonal (right) targets.

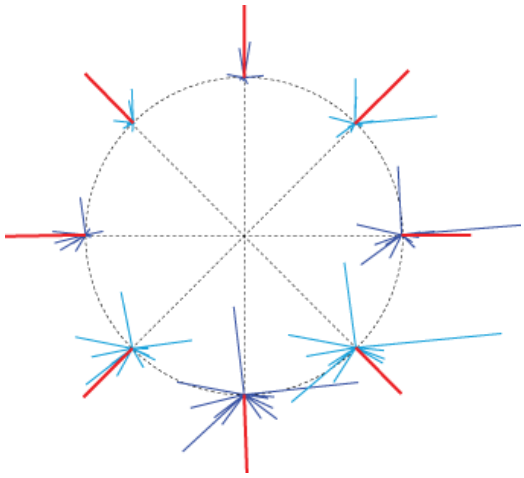

Figure 4. Contribution vectors from successful trials (244 of 320) of one session (9). Each of the 8 clusters of vectors (dark and light blue) around the circle represents the averaged control signal contribution across the duration of the reach per electrode for all trials at that target location. The red vector represents the net contribution of all electrodes for that target type.

IV. Discussion

Electrocorticography requires surgical implantation of recording electrodes, but is less prone to adverse tissue response than penetrating electrodes, and likely offers long-term stability for neural recording [8][23], making it an attractive modality for BCI applications. In order to be viable, however, it must be learnable for the user as well as reliable over the long term.

Consistent with previous results [10], we found that proficiency in the center-out task was achieved within 5 days. In this study, we employed a training strategy with a gradually updated decoder. While continuous updating of decoder weights could result in a shifting neural-to-kinematic mapping that the monkey could not master, gradual co-adaptation may assist acquisition of control by better matching the decoder to the neural signals as they change during the learning process.

Long-term stability of ECoG recording has been demonstrated previously. Chao et al. [8] showed that an offline decoder could reliably predict movement kinematics from ECoG signals for several months following initial training. Here we extend this finding with the use of an online decoder trained in the context of a closed-loop task. The monkey learned to move a cursor by modulating neural activity, and the association between intended movement and neural modulation remained stable for approximately 4 weeks and was reliably captured by our ECoG grid. This was evident from the observations that the success rate remained high, and that the computed vectors remained highly correlated with correct movement direction.

Regarding the organization of controlling neural features, this study shows preliminary evidence of a mixed control strategy that varied by direction. We found that targets requiring movement down or right had contribution vectors of larger magnitudes and wider distribution than targets up or left. This behavior (Fig. 4) suggests that the monkey's chosen control scheme involves utilizing a main directional driver when applicable and attenuating its strength with opposing vectors, or else recruiting multiple lesser control features to achieve the same degree of strength and specificity in other directions. The ability to produce a net control signal from different distributions of component vectors suggests an underlying flexibility that could facilitate reliable, robust control over time.

References

[1] D.W. Moran. Evolution of brain–computer interface: action potentials, local field potentials and electrocorticograms. *Current Opinion in Neurobiology*, 20(6):741-745, Dec 2010.

[2] D.W. Moran, A.B. Schwartz. Motor cortical representation of speed and direction during reaching. *Journal of Neurophysiology*, 82(5):2676-2692, Nov 1999.

[3] L. Paninski, S. Shoham, M.R. Fellows, N.G. Hatsopoulos, J.P. Donoghue. Superlinear Population Encoding of Dynamic Hand Trajectory in Primary Motor Cortex. *Journal of Neuroscience*, 24(39):8551-8561, Sep 2004.

[4] L.R. Hochberg, M.D. Serruya, G.M. Friehs, J.A. Mukand, M. Saleh, A.H. Caplan, A. Branner, D. Chen, R.D. Penn, J.P. Donoghue. Neuronal ensemble control of prosthetic devices by a human with tetraplegia. *Nature*, 442(7099):164-71, Jul 2006.

[5] W. Wang, S.S. Chan, D.A. Heldman, D.W. Moran. Motor cortical representation of position and velocity during reaching. *Journal of Neurophysiology*, 97(6):4258-4270, Jun 2007.

[6] C. A. Chestek, A. P. Batista, G. Santhanam, B.M. Yu, A. Afshar, J.P. Cunningham, V. Gilja, S.I. Ryu, M.M. Churchland, K.V. Shenoy: Single-neuron stability during repeated reaching in macaque premotor cortex. *Journal of Neuroscience*, 27(40):10742-50, Oct 2007.

[7] G. Schalk, K.J. Miller, N.R. Anderson, J.A. Wilson, M.D. Smyth, J.G. Ojemann, D.W. Moran, J.R. Wolpaw, E.C. Leuthardt. Two-dimensional movement control using electrocorticographic signals in humans. *Journal of Neural Engineering*, 5(1):75-84, Mar 2008.

[8] Z.C. Chao, Y. Nagasaka, N. Fujii. Long-term asynchronous decoding of arm motion using electrocorticographic signals in monkeys. *Frontiers in Neuroengineering*, 3:3, Mar 2010.

[9] E.C. Leuthardt, G. Schalk, J.R. Wolpaw, J.G. Ojemann, D.W. Moran: A brain–computer interface using electrocorticographic signals in humans. *Journal of Neural Engineering*, 1(2):63-71, Jun 2004.

[10] A.G. Rouse, D.W. Moran. Neural adaptation of epidural electrocorticographic (EECoG) signals during closed-loop brain computer interface (BCI) tasks. *Conference Proceedings: IEEE Engineering in Medicine and Biology Society Conference*, 5514-7, Sep 2009.

[11] G. Schalk, J. Kubánek, K.J. Miller, N.R. Anderson, E.C. Leuthardt, J.G. Ojemann, D. Limbrick, D. Moran, L.A. Gerhardt, J.R. Wolpaw. Decoding two-dimensional movement trajectories using electrocorticographic signals in humans. *Journal of Neural Engineering*, 4(3):264-275, Sep 2007.

[12] E.A. Felton, J.A. Wilson, J.C. Williams, P.C. Garell. Electrocorticographically controlled brain–computer interfaces using motor and sensory imagery in patients with temporary subdural electrode implants. *Journal of Neurosurgery: Pediatrics*, 106(3):495-500, Mar 2007.

[13] T. Pistohl, T. Ball, A. Schulze-Bonhage, A. Aertsen, C. Mehring. Prediction of arm movement trajectories from ECoG-recordings in humans. *Journal of Neuroscience Methods* 167(1):105-14, Jan 2008.

[14] W. Wang, A.D. Degenhart, J.L. Collinger, R. Vinjamuri, G.P. Sudre, P.D. Adelson, D.L. Holder, E.C. Leuthardt, D.W. Moran, M.L. Boninger, A.B. Schwartz, D.J. Crammond, E.C. Tyler-Kabara, D.J. Weber. Human motor cortical activity recorded with Micro-ECoG electrodes, during individual finger movements. *Conference Proceedings: IEEE Engineering in Medicine and Biology Society Conference*, 586-9, Sep 2009.

[15] M.S. Fifer, M. Mollazadeh, S. Acharya, N.V. Thakor, N.E. Crone. Asynchronous decoding of grasp aperture from human ECoG during a reach-to-grasp task. *Conference Proceedings: IEEE Engineering in Medicine and Biology Society Conference*, 4584-7, 2011.

[16] A.D. Degenhart, J.W. Kelly, R.C. Ashmore, J.L. Collinger, E.C. Tyler-Kabara, D. J. Weber, W. Wang. Craniux: a LabVIEW-based modular software framework for brain-machine interface research. *Computational Intelligence and Neuroscience*, 2011:363565, Apr 2011.

[17] E.A. Robinson. A historical perspective of spectrum estimation. *Proceedings of the IEEE*, 70(9):885-907, Sep 1982.

[18] N.E. Crone, D.L. Miglioretti, B. Gordon, R.P. Lesser. Functional mapping of human sensorimotor cortex with electrocorticographic spectral analysis. II. Event-related synchronization in the gamma band. *Brain* 121 (Pt 12): 2301-2315, Dec 1998.

[19] N.E. Crone, A. Sinai, A. Korzeniewska. High-frequency gamma oscillations and human brain mapping with electrocorticography. *Prog Brain Res* 159: 275-295, 2006.

[20] K.J. Miller, E.C. Leuthardt, G. Schalk, R.P. Rao, N.R. Anderson, D.W. Moran, J.W. Miller, J.G. Ojemann. Spectral changes in cortical surface potentials during motor movement. *J Neurosci* 27: 2424-2432, Feb 2007.

[21] E. Salinas, L.F. Abbott. Vector reconstruction from firing rates. *Journal of Computational Neuroscience*, 1(1-2):89-107, Jun 1994.

[22] J.J. Wheeler, D.W. Moran. Personal communication on adaptation of neural decoding weights for an ECoG-BCI experiment in a non-human primate. Washington University in St. Louis; 2011.

[23] E. Margalit, J.D. Weiland, R.E. Clatterbuck, G.Y. Fujii, M. Maia, M. Tameesh, G. Torres, S.A. D'Anna, S. Desai, D.V. Piyathaisere, A. Olivie, E. de Juan Jr, M.S. Humayunb. Visual and electrical evoked response recorded from subdural electrodes implanted above the visual cortex in normal dogs under two methods of anesthesia. *Journal of Neuroscience Methods*, 123(2):129–137, Mar 2003.